[CONTRIBUTION FROM THE INSTITUTE FOR ATOMIC RESEARCH AND DEPARTMENT OF CHEMISTRY, IOWA STATE COLLEGE]

On the Crystal Structures of the Magnus Salts, $Pt(NH_3)_4PtCl_4$[1]

BY MASAO ATOJI, JAMES W. RICHARDSON AND R. E. RUNDLE

RECEIVED FEBRUARY 9, 1957

The crystal structure of the Magnus green salt, $Pt(NH_3)_4PtCl_4$, is tetragonal, a = 9.03 Å. and c = 6.49 Å., with space group D_{4h}^9–P4/mnc, and two formula units per unit cell, showing that the structure previously reported is incorrect. The planar $Pt(NH_3)_4^{++}$ and $PtCl_4^{--}$ ions are stacked over one another along the c-axis with Pt–Pt distance, $c/2$ = 3.25 Å. The bond distances of Pt–Cl = 2.34 Å. and Pt–N = 2.06 Å. are obtained with high accuracy by means of the generalized Fourier synthesis. The interatomic distances and the infrared spectrum indicate no significant NH . . . Cl hydrogen bonding in this compound. The comparison between the radial distribution functions of this salt and its isomeric pink salt reveals that there is no direct Pt–Pt contact in the Magnus pink salt, but other distances are comparable.

Introduction

The slightly soluble Magnus salts, Magnus green salt (MGS) and Magnus pink salt (MPS), result promptly from the mixing of solutions of K_2PtCl_4 and $Pt(NH_3)_4Cl_2$.[2] The reaction is capricious; which salt will result is as yet beyond control. The analysis of both salts is $Pt(NH_3)_4PtCl_4$, making the elucidation of their differences an interesting problem in chemical isomerism.

MGS has been studied previously by X-ray diffraction methods.[3] X-Ray rotation diagrams were indexed using a tetragonal unit cell with a = 6.29 Å. and c = 6.42 Å., and the suggested space group was C_4^1–P4. These results, as well as the structure, placing all $Pt(NH_3)_4^{++}$ groups in one layer and all $PtCl_4^{=}$ in the next, are found to be incorrect, though platinum positions are correct. Apparently, the former X-ray diagrams did not reveal the presence of very weak reflections.

The isomeric pink salt, MPS, was studied previously by the X-ray method,[3] but without any conclusive result regarding its color and its structural difference from MGS. The present study will show some details in this respect.

Methods and Results

The single crystal of MGS used in this study was a tetragonal needle, elongated along c. It approximated a cylinder 0.04 mm. in radius. Zero to sixth-level Weissenberg diagrams were taken by rotation about the needle axis, using Mo Kα and Cu Kα radiation. Precession diagrams, ($h0l$) and (hhl), were also obtained using Mo Kα radiation. The timed exposure and multiple film techniques were combined in both intensity determinations.

The lattice constants are: a = 9.03 ± 0.02 Å. and c = 6.49 ± 0.01 Å. The calculated density of 3.77 g./cc. for two formula units in the unit cell agrees with the average value of the experimental density, 3.7 g./cc.[3] Systematic extinctions of ($0kl$) with $k + l$ odd, (hhl) with l odd, lead to the space group D_{4h}^6–P4/mnc or C_{4v}^6–P4nc.

The appropriate Lorenz and polarization factors were employed for reduction of the visual intensity estimates to structure factors. Phillips correction[4] was applied. The best available atomic scattering factors were used for Pt,[5] Cl[6] and N.[7] No calculations were made involving hydrogen atoms.

In both of the space groups above, there are two sets of Pt atoms. In P4nc both occupy 00z, $\frac{1}{2}$ $\frac{1}{2}$ $\frac{1}{2}$ + z. In P4/mnc these positions with z-values of 0 and $\frac{1}{2}$ are required for the two sets. Since general reflections with $h + k = 2n$ and $l = 2n$ are very strong at low angles and show approximately normal decline of intensities, z-values of about 0 and $\frac{1}{2}$ are indicated. Point symmetries at Pt atoms are C_4 and C_{4h} for the two space groups, so that square planar ions in the planes z = 0 and $\frac{1}{2}$ are required for P4/mnc, and only slight deviations from this are reasonable for the lower space group.

Data from ($hk0$) are dominated by platinum scattering, and the Patterson projection onto (001) revealed only the Pt-Cl vectors. Data from (hkl) with l odd contain little or no platinum contributions (none if z = 0 and $\frac{1}{2}$) and are consequently of importance in determining positions of light atoms. The generalized Patterson projection[8] onto (001) using ($hk1$) data showed clearly both Pt–Cl and Pt–N vectors.

The light atom parameters were refined successively by means of the difference generalized Fourier-syntheses using ($hk1$) data. The final generalized electron density projection onto (001) is shown in Fig. 1. The peak positions were located by the twenty points graphical least square method. The final parameters obtained are listed in Table I. The observed and calculated structure factors for ($hk1$) and ($hk3$) reflections, which were found to contain no Pt atom contributions, are listed in Table III. The discrepancy factor, $\Sigma||F_o| - |F_c||/\Sigma|F_o|$ is 10.5% for these 89 reflections. The temperature factor

$$\exp\left\{-(B_1l^2 + B_2)\left(\frac{h^2 + k^2}{a^2} + \frac{l^2}{c^2}\right)\right\}$$

with B_1 = 0.13$_8$ Å.^{2} and B_2 = 1.06 Å.^{2}, has been applied.

TABLE I

	x	y	z
Cl	0.0563	0.2528	0.000
N	.5627	.7197	.000

(1) Contribution No. 510. Work was performed in the Ames Laboratory of the U. S. Atomic Energy Commission.

(2) Magnus, *Pogg. Ann.*, **14**, 242 (1828).

(3) E. G. Cox, F. W. Pinkard, W. Wardlaw and G. H. Preston, *J. Chem. Soc.*, 2527 (1932).

(4) D. C. Phillips, *Acta Cryst.*, **9**, 819 (1956).

(5) K. Umeda and Y. Tomishima, *J. Phys. Soc. Japan*, **10**, 753 (1955).

(6) H. Viervoll and O. Ögrim, *Acta Cryst.*, **2**, 227 (1949).

(7) J. Berghnis, I. M. Haanappel, M. Potters, B. O. Loopstra, H. McGillavry and A. L. Veenedaal, *ibid.*, **8**, 478 (1955).

(8) H. Lipson and W. Cochran, "The Determination of Crystal Structures," G. Bell and Sons, London, 1953, pp. 221–227.

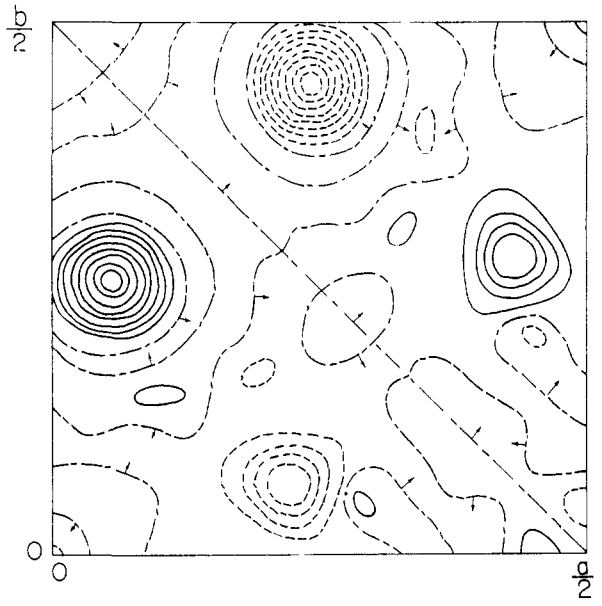

Fig. 1.—Generalized Fourier projection on (001) using (hkl) data. Contours are 0, 4, 8 . . . e.Å.$^{-2}$, but 0, 8, 16 . . . e.Å.$^{-2}$ for chlorine atoms. Positive, negative, zero contours are in solid, dotted and broken lines, respectively. Small arrows indicate the direction of the negative region.

Accuracy of the Structure.—Standard deviations of random errors were determined using Cruickshank's procedure,[9] which was modified appropriately for the generalized Fourier projection. For ($hk1$) data, $\sigma(A_h) = \sigma(A_k) = 1.624$ e.Å.$^{-3}$ and the peak constants are listed in Table II. The resultants, $\sigma(x) = \sigma(y) = 0.0037$ Å. for Cl and 0.018 Å. for N, give the standard deviations, 0.005 Å. for the Pt–Cl and 0.025 Å. for the Pt–N bond lengths.

TABLE II

OBSERVED AND CALCULATED PEAK CONSTANTS

	ρ_1(0)obsd. (e.Å.$^{-2}$)	ρ_1(0)calcd. (e.Å.$^{-2}$)		ρ_1''(0)obsd. (e.Å.$^{-4}$)	ρ_1''(0)calcd. (e.Å.$^{-4}$)	
N	10.2	11.4[a]	10.6[b]	− 92	−121[a]	− 92[b]
Cl	35.0	32.6	34.8	−440	−420	−440

[a] From equations 1 and 2. [b] From the generalized electron density map using the calculated structure factors.

The possibility that the structure was non-centrosymmetric was examined as follows. The peak height ρ_L (0) and the peak curvature ρ''_L (0) in the generalized Fourier projection along the z-axis, namely, using ($hk1$) data, are[10]

$$\rho_L(0) = \cos\left(2\pi\frac{LZ_0}{c}\right)\int_{L/c}^{s_{max}} 2\pi s f(s)\exp\left(-\frac{Bs^2}{4}\right)ds \quad (1)$$

and

$$\rho''_L(0) = \cos\left(2\pi\frac{LZ_0}{c}\right)\left[-\int_{L/c}^{s_{max}} 4\pi^3 s^3 f(s)\exp\left(-\frac{Bs^2}{4}\right)ds + \frac{2\pi^2L^2}{s^2}\rho_L(0)\right] \quad (2)$$

where z_0 is the atomic parameter in Å., c is the lattice constant along the z-axis, $f(s)$ is the atomic scattering factor and $s = 2(\sin\theta)/\lambda$. Although isotropic thermal vibrations are assumed in these equations, this should not cause the mean value of the observed peak constants to deviate greatly from the calculated value.[11] If $z = 0$ or $1/2$, $|\rho_L(0)|$ and $|\rho_L''(0)|$ give the maximum possible values. The graphically integrated results using equations 1 and 2 with $z = 0$, $B = 1.2$ Å.^{2}, $s_{max} = 1.275$ Å.$^{-1}$ and $L/c = 0.190$ Å.$^{-1}$ are listed in Table II. The chlorine peak constants are as high as expected for $z = 0$ or $1/2$, while those for the nitrogen atom may indicate some deviation. However, the latter peaks could be considerably affected by the Fourier ripple error. Moreover, the peak values in the observed and calculated Fourier maps are in good agreement, as can be seen in Table II. Ac-

(9) D. W. J. Cruickshank, *Acta Cryst.*, **2**, 65 (1949).
(10) M. Atoji, *ibid.*, in press.
(11) P. W. Higgs, *ibid.*, **6**, 232 (1953).

TABLE III

OBSERVED AND CALCULATED STRUCTURE FACTORS FOR ($hk1$) AND ($hk3$) ZONES

hkl	F_o	F_c	hkl	F_o	F_c
101	17.7	25.7	10,2,1	<4.0	2.2
301	30.3	27.1	11,2,1	14.6	15.0
501	16.7	−14.8	431	15.9	13.1
701	<4.8	− 2.3	531	65.7	69.0
901	26.0	−24.7	631	17.9	−16.0
11,0,1	3.6	− 3.5	731	6.0	− 5.4
211	32.0	−31.9	831	5.5	6.2
311	75.7	−75.6	931	16.6	13.8
411	27.5	25.4	10,3,1	13.7	−11.6
511	27.9	−29.1	541	<4.6	− 3.5
611	22.6	−22.1	641	7.2	6.5
711	26.0	−28.9	741	12.8	−13.5
811	21.3	22.4	841	<4.8	− 3.4
911	9.1	9.9	941	18.5	−16.0
10,1,1	20.5	−17.6	10,4,1	3.2	− 0.5
11,1,1	7.9	10.2	651	7.4	8.9
321	9.6	− 6.1	751	38.6	−37.6
421	10.1	− 8.9	851	<4.6	2.1
521	4.5	− 6.2	951	21.6	18.6
621	<5.0	2.4	10,5,1	6.0	7.3
721	20.0	21.3	761	8.3	8.8
821	<5.0	− 2.2	861	<4.2	− 0.5
921	6.2	9.5	961	18.6	19.3
871	21.5	−19.5	10,2,3	<1.8	1.3
971	7.6	8.1	433	10.8	10.0
103	18.5	17.2	533	46.0	50.0
303	22.4	18.4	633	11.8	−11.3
503	10.3	−10.4	733	3.1	− 3.8
703	<2.8	− 2.2	833	2.9	4.2
903	17.1	−16.0	933	9.7	8.7
213	21.7	−22.3	10,3,3	7.2	− 6.8
313	50.7	−50.4	543	4.5	− 2.7
413	19.7	19.3	643	5.0	4.3
513	16.8	−20.7	743	9.0	− 9.3
613	15.2	−16.5	843	4.7	− 2.1
713	16.5	−20.3	943	10.8	− 9.8
813	14.8	15.2	653	3.4	6.0
913	5.8	6.4	753	27.9	−24.8
10,1,3	14.1	−10.6	853	<2.6	1.3
323	8.6	− 5.6	953	11.9	11.1
423	6.2	− 5.3	763	6.6	5.7
523	4.0	− 3.7	863	<1.8	− 0.3
623	<2.8	1.5	873	10.0	−11.4
723	14.0	15.0			
823	<2.8	− 1.4			
923	4.3	6.2			

cordingly, no definite conclusion was deduced from these data.

In the series of generalized $(F_0 - F_c)$ Fourier maps, the origin peak was always negative. In the final difference map, only the origin showed a density value larger than 1 e.Å.$^{-2}$, namely, 1.88 e.Å.$^{-2}$. $\rho_1(0)$ of equation 1 is 196 e.Å.$^{-2}$ for the Pt atom. Therefore, the separation of Pt atoms along c needs to be changed from $c/2$ by only ± 0.013 Å. to account for peak height at the origin in the generalized difference map made from $(hk1)$ data and only 0.003 Å. in the map made from $(hk3)$ data. Similar calculations were carried out for the peak curvatures with similar results. It is our conclusion that the experimental data do not disagree with the proposed centrosymmetric structure within the limits of ± 0.02 Å. in the z-parameters.

Radial Distribution Studies.—Since no success was met in obtaining a sufficiently large single crystal of MPS for single crystal diffraction work, the integrated intensities of the Debye–Scherrer lines of both MGS and MPS were measured on a Norelco X-ray diffractometer. Although the average particle size of the powdered crystals was less than 5 μ the preferred orientation effect was not avoidable by the usual mounting technique.[12] Moreover, the mica-like cleavage of the pink salt raises great difficulty in obtaining finer powders with spherical or random shapes. However, it was observed that by mixing and diluting MPS with a considerable amount of granular starch the preferred orientation effect was reduced appreciably. The absolute intensities were obtained approximately by scanning the diffraction lines of the powdered mixture of these salts and NaCl.

The radial distribution function derived by Schomaker[13]

$$A(r) = \sum_{s>0}^{s_{max}} \frac{\sin 2\theta}{1 + \cos^2 2\theta} I(s) \exp(-Bs^2) \sin 2\pi sr$$

where $I(s)$ is the observed intensity, was summed at intervals of 0.1 Å. in r. In our case, s_{max} was 0.8 Å.$^{-1}$, and summations made with and without an artificial temperature factor were similar in main details. In the resultant distribution functions, as shown in Fig. 3, with $B = 8$ Å.$^{-2}$, Pt–Cl peaks I and I′ appeared in both salts, while the shortest Pt–Pt interaction, II, in MGS was not observed in MPS. Since there existed many ambiguities in interpreting peak III′, attempts to solve the structure of MPS from the radial distribution function failed. Nevertheless, it may be concluded that in MPS there is no direct contact of Pt atoms as found in MGS, and that in MPS the smallest Pt–Pt vectors lie under peak III′ at about 5.6 Å.

(12) H. P. Klug and L. E. Alexander, "X-Ray Diffraction Procedures," John Wiley and Sons, Inc., New York, N. Y., 1954, pp. 290–305.

(13) J. Waser and V. Schomaker, THIS JOURNAL, **67**, 2014 (1945). The correct expression to define $A(r)$ is as follows: If we define

$$D(r) = \int_0^{2\pi}\int_0^{\pi} P(\vec{r}) \sin\theta \, d\theta \, d\phi$$

where $P(r)$ is the Patterson function, we have then

$$A(r) = \frac{2rV}{\lambda}\left[D(r) - \frac{4\pi}{V} F^2(000)\right]$$

where V is the volume of the unit cell.

Discussion of Structure

In MGS, Pt–Cl = 2.34 Å. and Pt–N = 2.06 Å. are in good agreement with the sum of the covalent radii, Pt–Cl = 2.31 Å. and Pt–N = 2.02 Å.[14,15] Other important interatomic distances are shown in Fig. 2. These indicate no strong hydrogen bonding in MGS. Moreover, the NH stretching frequencies recorded on the infrared spectrometer with a LiF prism are 3182 and 3277 cm.$^{-1}$ for symmetric and asymmetric vibrations, respectively. Although the corresponding frequencies of NH_3[16] are 3337 cm.$^{-1}$ and 3414 cm.$^{-1}$, these differences probably do not arise from strong hydrogen bonding for reasons previously reported.[17]

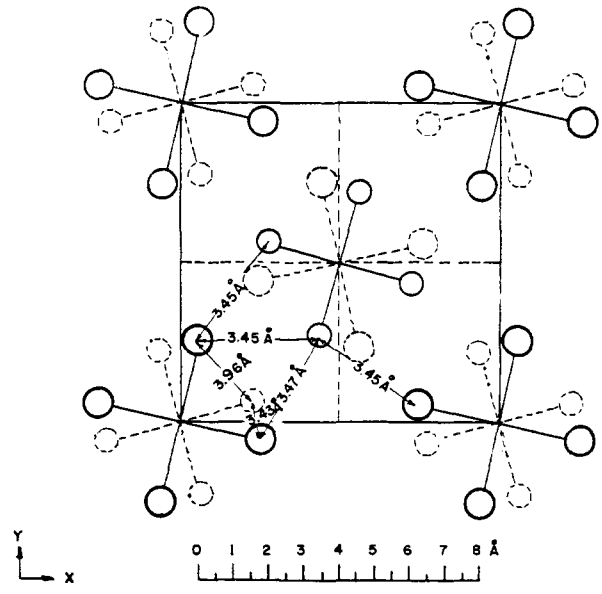

Fig. 2.—Atomic arrangement of the Magnus green salt projected on (001). Large circles represent chlorine atoms and small circles nitrogens. Solid and broken lines indicate $z = 0$ and $1/2$, respectively. Platinum atoms are at centers of square ions.

Remarkable dichroism of a single crystal of MGS was observed in the visible and ultraviolet region by Yamada.[18] His result and the chains of Pt atoms along the c-axis with a distance of 3.25 Å. suggested to him that there exists an interaction among Pt atoms. This seems to occur frequently in all square planar complexes except those of copper(II).[19] In valence bond terms the interaction can possibly be described as a slight mixing of octahedral with the square planar bonding with two of the octahedral bonds to adjoining metal atoms,[19a] or in molecular

(14) L. Pauling and M. L. Huggins, *Z. Krist.*, **87**, 205 (1934).

(15) Pt^{++}–Cl bond distances previously reported, but less exactly determined, are: in K_2PtCl_4, 2.32 Å. (R. G. Dickinson, THIS JOURNAL, **44**, 2404 (1922)), in $K(PtCl_3 \cdot C_2H_4)H_2O$, 2.32 Å. (J. A. Wunderlick and D. P. Mellor, *Acta Cryst.*, **7**, 130 (1954)). The Pt^{++}–N bond distance in $Pt(NH_3)_2Br_2$ is 2.16 Å. (C. Brosset, *Arkiv Kemi Min. Geol.*, **25A**, No. 19 (1948)).

(16) G. Herzberg, "Infrared and Raman Spectra of Polyatomic Molecules," D. Van Nostrand Co., New York, N. Y., 1945, p. 197.

(17) K. Nakamoto, M. Margoshes and R. E. Rundle, THIS JOURNAL, **77**, 6480 (1955).

(18) S. Yamada, *ibid.*, **73**, 1579 (1951).

(19) (a) L. E. Godycki and R. E. Rundle, *Acta Cryst.*, **6**, 487 (1953); R. Rundle, THIS JOURNAL, **76**, 3101 (1954); (b) R. Rundle, *J. Phys. Chem.*, **61**, 45 (1957).

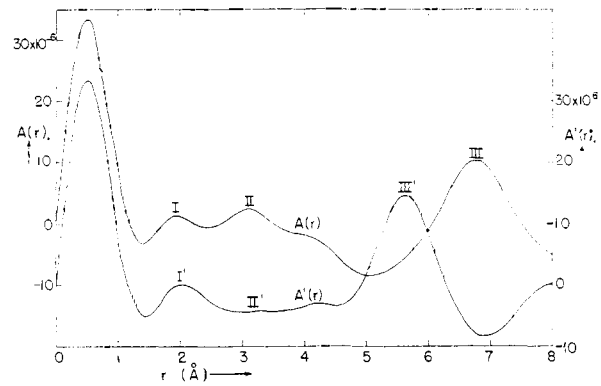

Fig. 3.—Radial distribution function of the Magnus green salt, $A(r)$, and of Magnus pink salt, $A'(r)$.

orbital terms as a configuration interaction involvgni some metal–metal bonding.[19b] The closest distance between Pt atoms in MPS would not be less than 5 Å. as seen from peak III′ in Fig. 3. The remarkable colors of MGS must result from the metal interaction, while MPS, which has no such interaction, does not differ materially in color from finely divided $Pt(NH_3)_4Cl_2$, and its pink color must be due to $Pt(NH_3)_4^{++}$ ions. Experimentally there is little doubt that MGS is the stable form of the Magnus salts, and this may be due to the extra metal interaction. Presumably accidents of nucleation produce the pink salt, but it may well be that packing considerations, by themselves, would favor the pink salt since the type of packing in the green salt is rare. It would also be interesting to learn whether there is an appreciable activation energy for forming the Pt–Pt bond in the green salt.

Acknowledgments.—The authors wish to express their thanks to Messrs. Russell A. Bonham and Peter Vossos for their assistance in some of the numerical computations and to Mr. E. Miller Layton for obtaining the infrared spectra. Dr. Don S. Martin and his students kindly supplied MGS and MPS, and contributed to our interest in this problem.

AMES, IOWA

[CONTRIBUTION NO. 511 FROM THE INSTITUTE FOR ATOMIC RESEARCH AND DEPARTMENT OF CHEMISTRY, IOWA STATE COLLEGE]

The Solubility of the Post-Transition Metals in their Molten Halides[1]

BY JOHN D. CORBETT, SAMUEL VON WINBUSH AND FRANK C. ALBERS

RECEIVED FEBRUARY 20, 1957

The solubilities of the respective metals in molten PbI_2, $SbCl_3$, SbI_3, $ZnCl_2$, ZnI_2, CdI_2 and $GaBr_2$ are reported. An interpretation of the solution of the post-transition representative metals in their molten halides is presented in terms of the formation of slightly stable subhalides. The apparent stabilities of the lower halides increase both with increasing atomic weight of the metal within a group, and with increasing atomic weight of the halide with a given metal, except for cadmium. The halide effect is attributed to a corresponding decrease in the extent to which the higher oxidation state of the metal is stabilized by complex formation with halide. The relative stabilities of the metal-halide complexes observed parallel those reported in aqueous solution for the same ions, including the inversion in order found for cadmium. The formation of gaseous subhalides of antimony, bismuth and gallium is indicated by transport experiments. A direct correspondence is found between those systems in which gaseous subhalides of appreciable stability are formed and those in which metal dissolves in the molten salt to an appreciable extent. Diamagnetic solutes are formed in the zinc, cadmium, gallium, antimony and bismuth systems.

Introduction

The problem presented by the apparent solution of such metals as cadmium,[2] bismuth,[3] cerium,[4] the alkalies,[5,6] and the alkaline earths[7] in their respective molten halides has not received a completely satisfactory explanation. Although the possibility of the formation of colloidal metal or "pyrosoles" in the process has been eliminated, interpretations in terms of energy bands for the metal's electrons,[8] the formation of subhalides,[2,3,9] or a combination of these concepts[5] has been suggested. The phenomenon appears to be limited to the liquid state, in that only an intimate mixture of the original components is obtained on solidification of these solutions.

Although generally small metal solubilities had been found previously in this Laboratory for lead, tin, aluminum, thallium and silver systems,[10] subsequent investigations have revealed larger interactions in other post-transition metal–metal halide melts. In addition, evidence has been obtained supporting the interpretation of these solubilities in terms of the formation of slightly stable lower halides.

Results

The data obtained are given in Table I. The number of significant figures reported is indicative of the reproducibility of the measurement. In the liquid state only the Cd–CdI_2 system is different in color from the pure salt. The resulting solids are quite distinctive, however, for all but the Pb–PbI_2 and Zn–$ZnCl_2$ systems at the lowest temperatures

(1) Presented in part at the 129th meeting of the American Chemical Society, Dallas, Texas, April 12, 1956. Work was performed in the Ames Laboratory of the U. S. Atomic Energy Commission.

(2) G. von Hevesy and E. Löwenstein, *Z. anorg. allgem. Chem.*, **187**, 266 (1930).

(3) B. Eggink, *Z. physik. Chem.*, **64**, 449 (1908).

(4) D. Cubicciotti, THIS JOURNAL, **71**, 4119 (1949).

(5) M. A. Bredig, J. W. Johnson and W. T. Smith, *ibid.*, **77**, 307 (1955).

(6) M. A. Bredig, H. R. Bronstein and W. T. Smith, *ibid.*, **77**, 1454 (1955).

(7) D. D. Cubicciotti and C. D. Thurmond, *ibid.*, **71**, 2149 (1949).

(8) D. D. Cubicciotti, *ibid.*, **74**, 1198 (1952).

(9) K. Grjotheim, F. Grönvold and J. Krogh-Moe, *ibid.*, **77**, 5824 (1955).

(10) J. D. Corbett and S. von Winbush, *ibid.*, **77**, 3964 (1955).